

# Blood flow and oxygen consumption with near-infrared spectroscopy and venous occlusion: spatial maps and the effect of time and pressure of inflation

**Claudia Casavola**

Laboratory for Fluorescence Dynamics  
Department of Physics  
University of Illinois at Urbana-Champaign  
1110 West Green Street  
Urbana, Illinois 61801-3080  
and  
Università degli Studi di Bari  
Dipartimento di Fisica  
Via E. Orabona, 4, I-70126  
Bari, Italy

**Lelia Adelina Paunescu**

**Sergio Fantini**

**Enrico Gratton**

Laboratory for Fluorescence Dynamics  
Department of Physics  
University of Illinois at Urbana-Champaign  
1110 West Green Street  
Urbana, Illinois 61801-3080

**Abstract.** We have measured the local blood flow (BF) and oxygen consumption (OC) in the human calf muscle using near-infrared spectroscopy during venous occlusion. Venous occlusion was achieved by inflating a pneumatic cuff around the thigh of the subject. We have investigated the influence of the inflation time and cuff pressure on the recovered values of BF and OC. We have found that if the cuff pressure is increased from a threshold pressure ( $\sim 30$  mm Hg) to a critical pressure ( $\sim 45$  mm Hg) in less than about 6 s, one measures the same values of BF and OC independent of the total inflation time and final cuff pressure. We also report nine-pixel spatial maps of BF and OC to show that this technique can lead to spatially resolved measurements of blood flow and oxygen consumption in tissues.  
© 2000 Society of Photo-Optical Instrumentation Engineers. [S1083-3668(00)00903-5]

**Keywords:** near-infrared spectroscopy; venous occlusion; blood flow; oxygen consumption.

Paper 42017 JBO received Sep. 15, 1999; revised manuscript received Feb. 4, 2000; accepted for publication Apr. 13, 2000.

## 1 Introduction

Local blood flow (BF), expressed in ml of blood per 100 ml of tissue per minute, and oxygen consumption (OC), expressed in  $\mu\text{mol}$  of  $\text{O}_2$  per 100 ml of tissue per minute, are relevant physiological parameters. Both the BF and the OC can experience temporal or spatial variations in response to endogenous (by substances that induce vasodilatation or vasoconstriction)<sup>1,2</sup> and exogenous (by drug intake) stimuli.<sup>3</sup> Consequently, a measurement of the spatial distribution of BF and OC in skeletal muscles can be a valuable tool to study metabolic and physiological processes. Near-infrared spectroscopy (NIRS) can be used to measure local blood flow and oxygen consumption, noninvasively, and *in situ*. NIRS measures tissue blood flow using different protocols such as the modulation of the fraction of inspired oxygen ( $\text{FiO}_2$ ),<sup>4</sup> the venous occlusion,<sup>4–7</sup> and the tilting table.<sup>8–11</sup> These protocols are noninvasive, cause no discomfort, and allow simultaneous measurements of local blood flow and oxygen consumption in skeletal muscles. Moreover, the modulation of the fraction of inspired oxygen and tilting table protocols can be used for brain investigation. Reported values of rest blood flow in skeletal muscles, measured with NIRS, are in the range 0.1–5.3 ml/100 ml/min.<sup>4–6,12</sup> *In situ* muscle oxygen consumption can be measured by NIRS during arterial occlusion.<sup>5,13</sup> In fact, the increase in deoxy-hemoglobin during arterial occlusion can be attributed to the conversion of oxy-hemoglobin into deoxy-hemoglobin. Alternatively, one can measure the muscle oxy-

gen consumption locally and noninvasively using the above mentioned protocols based on the modulation of the fraction of inspired oxygen, the venous occlusion, and the tilting table. Reported values of muscle oxygen consumption at rest are in the range 1.8–12.3  $\mu\text{mol}/100$  ml/min.<sup>5,14</sup> By measuring at rest we mean that the protocol does not involve the application of any particular stress to the measured tissue. In measurements at rest, the subject is lying or sitting motionless and no exercise is required.

We have applied the venous occlusion protocol to measure the local blood flow and oxygen consumption in the human calf muscle using NIRS. In particular, we have investigated the effect of different inflation times and cuff pressures in the venous occlusion protocol. We also report changes in the optical scattering properties of skeletal muscles during venous occlusion. Finally, we demonstrate how NIRS can provide spatial maps of blood flow and oxygen consumption in the calf muscle of a human subject.

## 2 Methods

### 2.1 Tissue Spectrometer

The optical measurements were performed using a dual wavelength, frequency-domain, multidistance, near-infrared spectrometer (Model No. 96208, ISS, Inc., Champaign, IL).<sup>15</sup> The experimental arrangement is depicted in Figure 1. The light sources consist of eight laser diodes, four emitting at 758 nm and four at 830 nm. The average power of the laser diodes is a few mW. The intensity of the laser diodes is sinusoidally modulated at a frequency of 110 MHz, and the laser diodes are multiplexed at a rate of 50 Hz so that each one of them is on for 20 ms. The laser diodes are coupled to optical fibers,

The present address of Sergio Fantini is: Bioengineering Center, Department of Electrical Engineering and Computer Science, Tufts University, 4 Colby Street, Medford, MA 02155.

Address all correspondence to Lelia Adelina Paunescu. Tel: 217-244-5620; Fax: 217-244-7187; E-mail: lpaunesc@uiuc.edu

This paper was originally scheduled to appear in the April 2000 special issue honoring Britton Chance, but was not available in time.

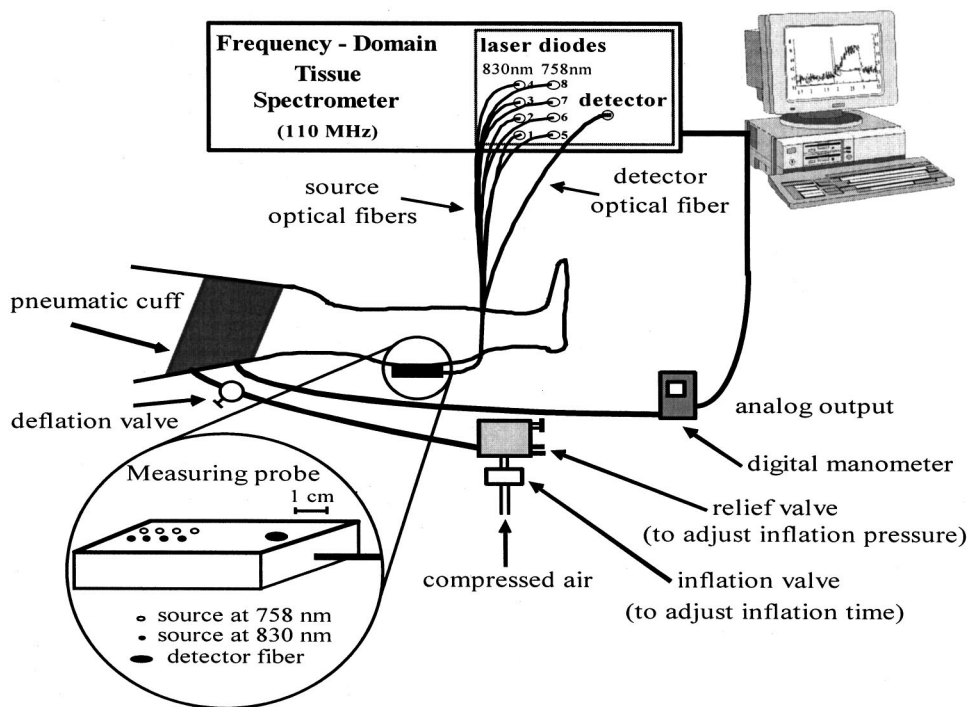


Fig. 1 Experimental setup.

with a core diameter of 400  $\mu\text{m}$ , that guide the light to the tissue. The light emitted by the laser diodes propagates through the tissue, and part of this light is diffusely reflected through the skin. An optical fiber bundle (3 mm in internal diameter) collects the diffusely reflected light that has propagated through the tissue and delivers it to a photomultiplier tube detector (PMT). The PMT gain is modulated at a frequency differing by 5 kHz from the modulation frequency of the light sources. This achieves the down conversion of the 110 MHz signal to 5 kHz. A fast Fourier transform of the 5 kHz signal provides the direct component (DC), the alternating component (AC) and the phase  $\Phi$  of the high frequency signal.<sup>16</sup>

The optical probe containing the source fibers was located on the posterolateral aspect of the gastrocnemius muscle. The source fiber tips corresponding to the eight laser diodes are placed at distances between 2 and 3.5 cm, respectively, from the detector fiber, with a constant increment of 0.5 cm, as shown in the inset of Figure 1.

## 2.2 Measurement of Hemoglobin Concentration and Saturation

The tissue optical parameters, namely the absorption coefficient  $\mu_a(\lambda)$  and the reduced scattering coefficient  $\mu'_s(\lambda)$ , can be calculated from the measured DC, AC, and  $\Phi$  according to diffusion theory. In the semi-infinite geometry, diffusion theory leads to expressions<sup>17</sup> that can be approximated (for  $r\sqrt{3\mu_a\mu'_s} \gg 1$ ) as follows:

$$\ln(r^2\text{DC}) = rS_{\text{DC}}(\mu_a, \mu'_s) + K_{\text{DC}}, \quad (1)$$

$$\ln(r^2\text{AC}) = rS_{\text{AC}}(\mu_a, \mu'_s) + K_{\text{AC}} \quad (2)$$

$$\Phi = rS_{\Phi}(\mu_a, \mu'_s) + K_{\Phi}, \quad (3)$$

where  $S_{\text{DC}}$ ,  $S_{\text{AC}}$ , and  $S_{\Phi}$  represent the slopes of the straight lines given by the  $\ln(r^2\text{DC})$ ,  $\ln(r^2\text{AC})$ , and  $\Phi$ , respectively, as a function of source–detector distance  $r$ , and  $K_{\text{DC}}$ ,  $K_{\text{AC}}$ ,  $K_{\Phi}$  are quantities independent of  $r$ . Therefore, in our multi-distance configuration,  $\mu_a(\lambda)$  and  $\mu'_s(\lambda)$  can be calculated from the slopes of two of the three measured quantities (DC, AC, and  $\Phi$ ). Since the DC reading can be affected by room light, we used the AC and the  $\Phi$  parameters to obtain the optical coefficients. Once  $\mu_a$  and  $\mu'_s$  have been measured at two wavelengths, it is possible to calculate the concentrations of oxy-, deoxy-, and total hemoglobin, which are expressed in  $\mu\text{M}$ . In fact, the dominant contribution to the optical absorption in tissues comes from hemoglobin, myoglobin, and water. The concentration of myoglobin in muscles is typically lower than that of hemoglobin,<sup>18</sup> and its contribution to the optical absorption will be neglected in this paper. We have taken into account the water absorption in tissues by subtracting  $0.7\mu_a^{\text{H}_2\text{O}}(\lambda)$  (with  $\mu_a^{\text{H}_2\text{O}}$  absorption coefficient of water) from the measured value of the absorption coefficient ( $\mu_a(\lambda)$ ). We have chosen the factor 0.7 in the water-correction term because the average water content in skeletal muscle is 70%.<sup>19</sup> The oxy- and deoxy-hemoglobin concentrations are given by<sup>17</sup>

$$[\text{HbO}_2] = \frac{\mu_a^*(\lambda_1)\epsilon_{\text{Hb}}(\lambda_2) - \mu_a^*(\lambda_2)\epsilon_{\text{Hb}}(\lambda_1)}{\epsilon_{\text{HbO}_2}(\lambda_1)\epsilon_{\text{Hb}}(\lambda_2) - \epsilon_{\text{HbO}_2}(\lambda_2)\epsilon_{\text{Hb}}(\lambda_1)}, \quad (4)$$

$$[\text{Hb}] = \frac{\mu_a^*(\lambda_2) \cdot \varepsilon_{\text{HbO}_2}(\lambda_1) - \mu_a^*(\lambda_1) \cdot \varepsilon_{\text{HbO}_2}(\lambda_2)}{\varepsilon_{\text{HbO}_2}(\lambda_1) \cdot \varepsilon_{\text{Hb}}(\lambda_2) - \varepsilon_{\text{HbO}_2}(\lambda_2) \cdot \varepsilon_{\text{Hb}}(\lambda_1)}, \quad (5)$$

where  $\mu_a^*(\lambda) = \mu_a(\lambda) - 0.7\mu_a^{\text{H}_2\text{O}}(\lambda)$  indicates the water-corrected absorption coefficient, while  $\varepsilon_{\text{Hb}}(\lambda)$  and  $\varepsilon_{\text{HbO}_2}(\lambda)$  are the molar extinction coefficients of deoxy- and oxy-hemoglobin, respectively. To apply Eqs. (4) and (5), we have used the values of  $\varepsilon_{\text{Hb}}(\lambda)$  and  $\varepsilon_{\text{HbO}_2}(\lambda)$  reported by Wray et al.<sup>20</sup> Finally, the hemoglobin saturation  $Y$  is defined as

$$Y = \frac{[\text{HbO}_2]}{[\text{Hb}] + [\text{HbO}_2]}. \quad (6)$$

During our measurement protocol, we record a set of values of  $\mu_a(\lambda)$ ,  $\mu_s'(\lambda)$ ,  $[\text{HbO}_2]$ ,  $[\text{Hb}]$ , and  $Y$  every 160 ms (20 ms/diode  $\times$  8 diodes). Since in this application we have studied hemodynamics occurring on a time scale of minutes, we have averaged four successive points to attain an acquisition time per data point of 0.64 s.

### 2.3 Venous Occlusion Protocol

In the venous occlusion protocol the subject was lying horizontally on a bed, and the optical probe of the near-infrared oximeter was positioned on the calf muscle (Figure 1). The feet of the subject were slightly lifted to allow the positioning of the probes on the posterolateral aspect of the calf. A pneumatic cuff was placed around the thigh of the subject. After the acquisition of a baseline, the cuff was inflated to a pressure of 60 mm Hg, or to a pressure in the range 20–100 mm Hg in the study of the effect of the cuff pressure (at 20 mm Hg, we did not observe significant changes in the hemoglobin concentration, so that the BF and OC were not measurable). This pressure was kept constant for 1 min and then quickly released by opening a deflation valve. The inflation of the pneumatic cuff was achieved by a high-pressure air line. The inflation time was varied by adjusting the aperture of an inflation valve. This inflation system affords adjustable inflation times down to a fraction of a second. A relief valve (Airtrol, Elmsford, NY, Part No. RV 5300-10) was used to set the cuff pressure to a predetermined value. The cuff pressure was continuously monitored by a digital manometer (Cole Parmer, Vernon Hills, IL, Part No. 68023-03). The manometer's analog output allowed the recording of the pressure value by the computer.

The systolic and diastolic pressures are the highest and lowest values of the arterial pressure wave, and their normal values are 120 and 80 mm Hg, respectively. A pressure in the range 20–100 mm Hg is below the normal value of systolic pressure and this means that the arterial blood flow should not be affected. For the case of pressure values above 100 mm Hg one might affect the arterial flow inducing a partial arterial occlusion. In our study, the subjects had normal systolic/diastolic pressure values.

Typical values of venous pressure in the calf muscle, in supine position, are 30 mm Hg.<sup>21</sup> Thus, if an external pressure of 30–60 mm Hg is applied to the thigh of the subject, the venous flow through the thigh is hindered. In our venous occlusion protocol, we chose a value of 60 mm Hg to induce a

venous occlusion because an external pressure 30 mm Hg higher than the typical vein pressure assures that the venous flow is interrupted.

### 2.4 Measurement of Blood Flow and Oxygen Consumption

Typical values of venous pressure are 30 mm Hg.<sup>21</sup> When an external pressure higher than venous pressure is applied to the thigh, the arterial inflow toward the calf is not affected, while the venous outflow is interrupted. This causes an increase in the blood volume of the calf, and an increase in the concentrations of oxy-, deoxy-, and total hemoglobin in the tissue. The initial rate of increase in the concentration of total hemoglobin (THC) in the calf muscle following the occlusion is proportional to the tissue BF,<sup>6</sup> and is given by

$$\text{BF} = \frac{1}{C} \frac{d[\text{THC}]}{dt}, \quad (7)$$

where  $C$  is the hemoglobin concentration in the blood.

The rate of increase in the deoxy-hemoglobin concentration during venous occlusion is due to the conversion of oxy- into deoxy-hemoglobin (which results from the tissue oxygen consumption), plus a term (usually smaller) given by the deoxygenated component of incoming arterial blood. Thus, the OC is given by

$$\text{OC} = 4 \frac{d}{dt} \left[ [\text{Hb}] - \frac{100 - \text{SaO}_2}{100} [\text{THC}] \right], \quad (8)$$

where the factor 4 accounts for the four molecules of oxygen bound to each molecule of oxy-hemoglobin, and  $\text{SaO}_2$  is the arterial saturation in percent.

The values of blood flow and oxygen consumption can be calculated by performing a linear regression of the temporal traces of  $[\text{Hb}]$  and  $\text{THC}$  following the onset of the occlusion. The limits of the interval for the regression were set as follows:

- the lower limit was determined by the point on the  $\text{THC}$  trace that corresponds to the first point above the  $\text{THC}$  baseline noise;
- the upper limit was determined by the onset of a significant deviation of the  $\text{THC}$  trace from linearity.

By substituting the temporal slopes of the initial increase of  $[\text{Hb}]$  and  $[\text{HbO}_2]$  into Eqs. (7) and (8) we can determine BF and OC. We note that in the calculation of blood flow and oxygen consumption, the contribution to the optical absorption from myoglobin is negligible. In fact, hemoglobin acts as an oxygen carrier and has a low oxygen affinity, so that oxygen is easily released to the tissue.<sup>22</sup> On the contrary, myoglobin acts as an oxygen reservoir in muscles, its oxygen affinity being considerably higher than that of hemoglobin. It is therefore reasonable to assume that the saturation of myoglobin in muscles remains constant, at rest. Since the calculation of blood flow and oxygen consumption considers the variations of the concentrations of oxy- and deoxy-hemoglobin with time, the contribution of myoglobin is expected to be minimal.

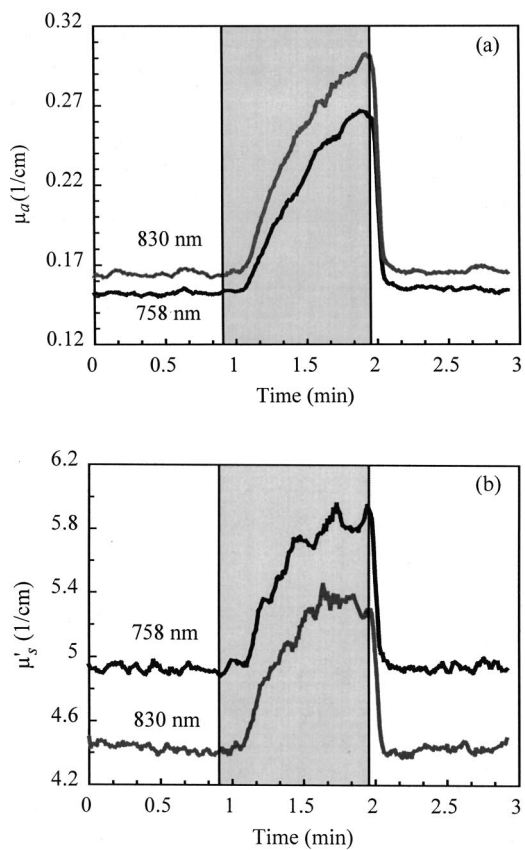


**Fig. 2** Time traces of: (a) absorption and (b) reduced scattering coefficients at the two wavelengths used (758 and 830 nm) as a function of time, during venous occlusion at 60 mm Hg pressure. The two vertical lines represent (1) the beginning of the inflation and (2) the deflation of the cuff. The shaded area represents the duration of the venous occlusion. The inflation time in this case was 1 s.

We have constructed spatial maps of blood flow and oxygen consumption on the calf muscle by measuring BF and OC at nine locations constituting a grid of 3×3 points, each point being separated by 0.5 cm from its neighbors. The measurement of a complete spatial map was obtained in about 25–30 min.

### 3 Results

Figure 2 shows the time traces of the tissue optical coefficients measured during venous occlusion on a healthy, 36 yr old, male subject. The increase in the optical absorption  $\mu_a(\lambda)$  [Figure 2(a)] results from the increase in blood volume during the venous occlusion. The significant increase in the reduced scattering coefficient  $\mu_s'(\lambda)$  [about  $0.9 \text{ cm}^{-1}$  in Figure 2(b)] is also mainly a result of the increase in blood volume. The increase in the scattering coefficient per unit hemoglobin concentration is  $0.016 \text{ cm}^{-1} \mu\text{M}^{-1}$ , in this case. To obtain a more statistically significant result, we have examined the scattering changes caused by venous occlusion in a population of 30 subjects. The average increase in the reduced scattering coefficient per unit hemoglobin concentration ( $\pm$  standard deviation) in these 30 subjects was  $0.023 \pm 0.013 \text{ cm}^{-1} \mu\text{M}^{-1}$ . This value was about the same at the

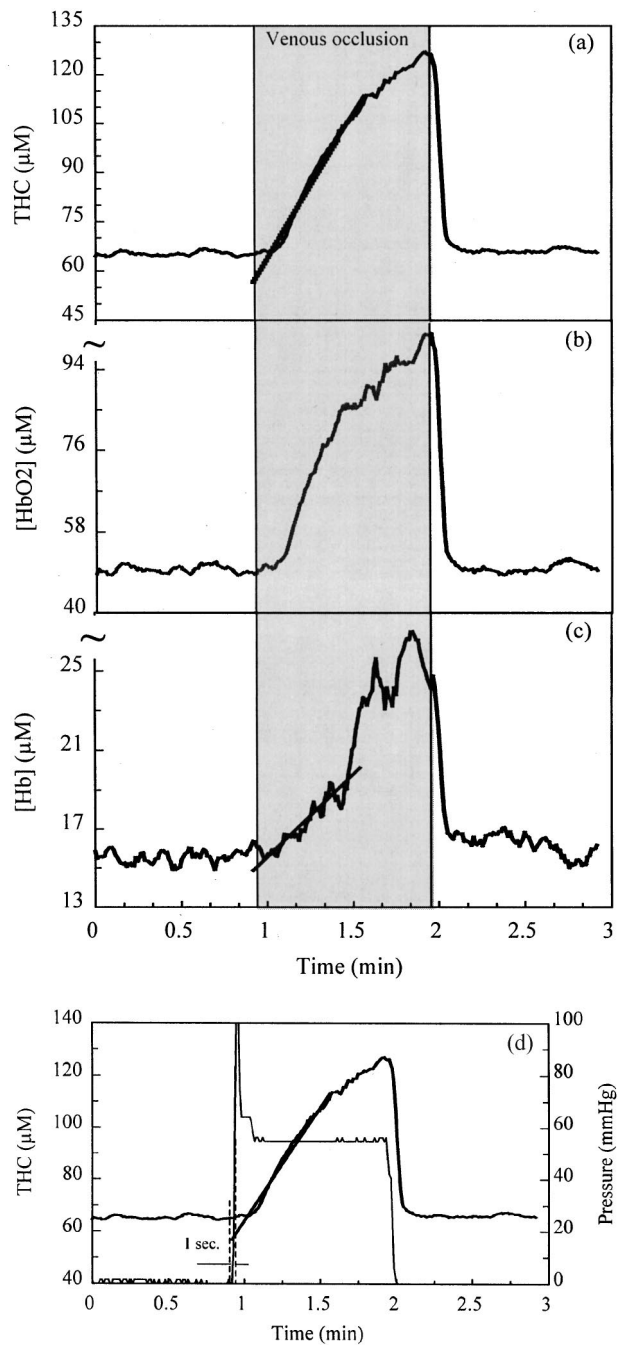


**Fig. 3** Time traces of: (a) total hemoglobin (THC), (b) oxy-hemoglobin ( $[\text{HbO}_2]$ ), (c) deoxy-hemoglobin ( $[\text{Hb}]$ ) concentrations, and (d) THC (left y axis) and cuff pressure (right y axis) during venous occlusion. The vertical lines in panels (a)–(c) have the same meaning as in Figure 2. The inflation time was 1 s. The results of the linear regressions used in the calculation of BF and OC are shown in panels (a) and (c). The corresponding values are  $\text{BF}=3.8 \pm 0.4 \text{ ml}/100\text{ml}/\text{min}$  and  $\text{OC}=2.3 \pm 0.9 \mu\text{mol}/100\text{ml}/\text{min}$ . The dotted lines in panel (d) represent the beginning and the end of the cuff inflation.

two wavelengths (758 and 830 nm). This result is consistent with the value of  $0.014 \pm 0.005 \text{ cm}^{-1} \mu\text{M}^{-1}$  measured in whole blood at 802 nm.<sup>23</sup>

Figures 3(a)–3(c) show the traces of oxy-, deoxy-, and total hemoglobin concentration during the venous occlusion

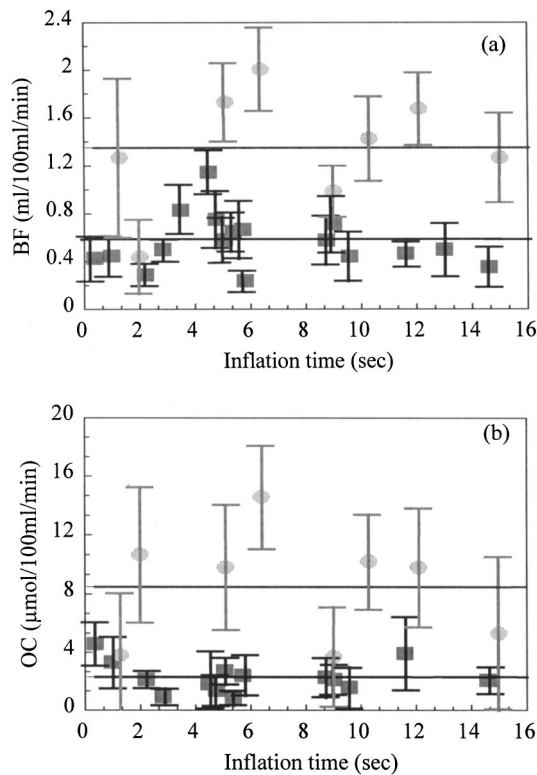


**Fig. 4** Measured values of: (a) blood flow (BF) and (b) oxygen consumption (OC) as a function of inflation time. The horizontal line in each panel represents the average of the calculated mean values of BF and OC. The error bars represent the standard deviation of the BF and OC values calculated from the linear regressions. The two symbols represent values of two different subjects.

protocol that are derived from the absorption traces of Figure 2(a), as described in Sec. 2.2. Both oxy- and deoxy-hemoglobin concentrations increase in response to the cuff inflation, and a saturation effect is reached when the increased blood pressure within the calf muscle balances the external pressure provided by the cuff. This saturation effect is not clearly seen in our measurements because the 1 min venous occlusion is not long enough to allow complete saturation. However, one can see that the traces have two different slopes during the 1 min venous occlusion, showing a tendency to saturate. Immediately after the deflation valve is opened, the concentrations recover the initial baseline values. One aspect of interest is whether, and how, the inflation time affects the measurement of blood flow and oxygen consumption. In principle, by including in the linear regression data points collected before a complete venous occlusion is achieved, one can introduce an error. We define the inflation time as the time interval from the instant when the cuff pressure is raised above the baseline noise, to the time when the desired pressure was reached by the leading edge of the pressure trace; for example, in Figure 3(d) the inflation time is 1 s.

We have measured the blood flow and oxygen consumption for different inflation times in the range 0.4–15 s. The recovered values of blood flow and oxygen consumption versus inflation time are shown in Figure 4 for two subjects. In the range of inflation times considered by us, we did not observe any significant dependence of the measured BF and OC

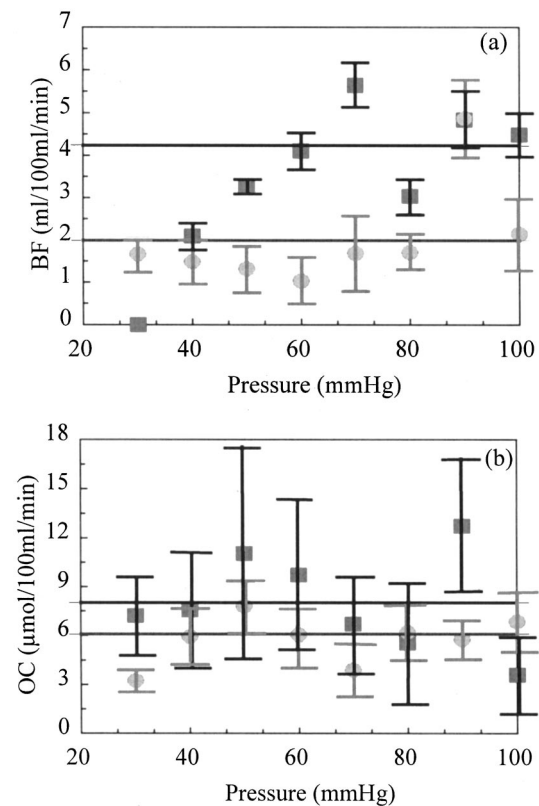


**Fig. 5** Measured values of: (a) blood flow (BF) and (b) oxygen consumption (OC) as a function of inflation pressure. The horizontal line in each panel represents the average of the measurements above 50 mm Hg. The error bars represent the standard deviation of the BF and OC values calculated from the linear regressions. The two symbols represent values of the same two subjects reported in Figure 4.

on the inflation time. We reproduced this result in one more subject.

Another aspect of interest is the effect of the inflation pressure on the measured values of blood flow and oxygen consumption. We calculated BF and OC as a function of the inflation pressure, in the range 30–100 mm Hg. The results are presented in Figure 5, which shows that pressures higher than about 45 mm Hg yield the same measured values of BF and OC. We reproduced this result in three more subjects, where the values of this critical pressure were in the range 30–45 mm Hg.

We define the critical pressure as the pressure above which the measured blood flow is independent of the applied cuff pressure. We also introduce a threshold pressure, defined as the minimum cuff pressure that induces an increase of the total hemoglobin concentration in the muscle. To measure the critical pressure and the threshold pressure more accurately, we repeated the measurements three times using cuff pressure values in the interval 15–60 mm Hg, by increments of 5 mm Hg. All these measurements were conducted on the same subject. These measurements indicated that a cuff pressure <30 mm Hg does not induce any increase in the muscle THC, while cuff pressures >30 mm Hg induce an increase of THC that is indicative of a partial or complete venous occlusion. Consequently, we assign a value of about 30 mm Hg to the threshold pressure.

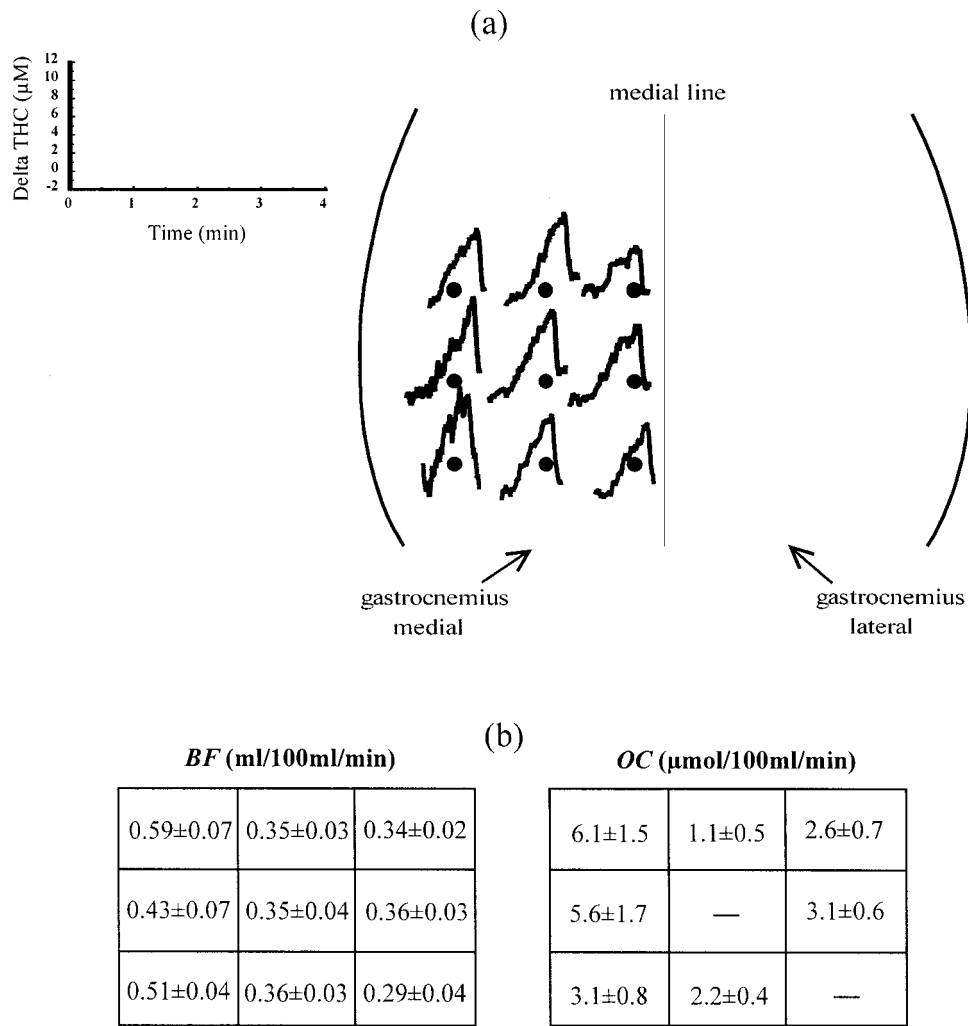


**Fig. 6** (a) The black circles represent the nine pixels of the spatial maps of blood flow and oxygen consumption measured on the gastrocnemius medial of the right calf muscle. The maps cover a 1 cm×1 cm area with a 0.5 cm increment. The traces represent the relative changes in THC during venous occlusion according to the coordinates shown in the top left corner. (b) The values of BF and OC at the nine pixels considered. In two pixels, the OC could not be calculated because of a low signal-to-noise ratio and are represented by the symbol “—.”

Figure 6 shows spatial maps of blood flow and oxygen consumption measured on the calf muscle. In general, the increase in the concentration of deoxy-hemoglobin during venous occlusion is on the order of 2–10  $\mu\text{M}$ , among different subjects, while the increase in the total hemoglobin concentration is about 10–70  $\mu\text{M}$ . The larger increase in total hemoglobin concentration with respect to deoxy-hemoglobin concentration accounts for a typically smaller error in the measurement of blood flow than in the measurement of oxygen consumption. In some cases, such as two pixels in the oxygen consumption map [Figure 6(b)], the OC values could not be calculated because the noise in the corresponding [Hb] traces was comparable with the occlusion-induced increase in [Hb].

Figure 7 shows the distributions of BF and OC values obtained by repeating the venous occlusion protocol 25 times in sequence on the same subject. As discussed above, the error in the measurement of OC is typically greater than the error in BF. The OC error was higher than 50% in 14 cases, while the BF error was higher than 50% in only two cases.

Figure 7 also shows that the variability of the measured BF and OC values on the same subject and at the same location is comparable to or greater than the spatial variability obtained in the BF and OC maps (Figure 6). A similar variability was also shown by other authors.<sup>5,14</sup> We observe that the blood flow and the oxygen consumption values reported in Figure 3, Figures 4 and 5 (data represented by squares) and Figure 6 measured on the same subject (but at different times). While the OC values reported in Figures 3–6 fall within the range of measurable values shown in Figure 7, this is not the case for the blood flow values. We attribute the origin of the wider range of BF values in Figures 3–6 with respect to Figure 7(a), to the physiological fluctuations of the blood flow values during the day. Blood flow and oxygen consumption can be affected by many factors such as gravitational stress, food ingestion, exercise, and environmental temperature.<sup>22,24,25</sup> It is known<sup>24,25</sup> that the ingestion of food and the meal size can affect the limb blood flow. In our study, we have measured the same subject at three different times during the day. We have chosen 10 am after a light breakfast, 2 pm immediately

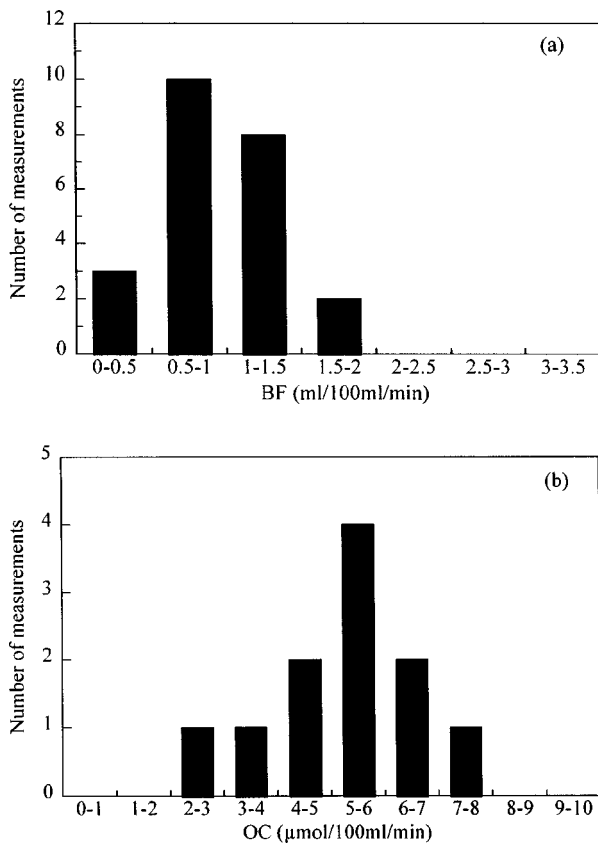


Fig. 7 Histograms of the distributions of: (a) BF and (b) OC measured in sequence on the same subject and at the same location.

after lunch, and 5 pm later after lunch. In these measurements, we found a range of BF values comparable to that of Figures 3–6.

#### 4 Discussion

The increase in the optical absorption during venous occlusion is a consequence of the increase in the concentration of hemoglobin in the tissue. The observed increase in the reduced scattering coefficient during the venous occlusion can be attributed, at least in part, to the increase in the number of red blood cells in the calf muscle during the occlusion. The increase in the reduced scattering coefficient is relevant because there are continuous wave (cw) near-infrared techniques that assume a constant scattering coefficient to quantify changes in absorption. We recalculated the values of blood flow and oxygen consumption by processing the DC data with the differential pathlength factor (DPF)<sup>26,27</sup> and DC slope<sup>28</sup> methods. We found that the values of BF measured with cw spectroscopy are consistently greater, by about 50%, than the corresponding values measured with frequency-domain data. The larger measurement error in OC resulted in a less significant difference between cw and frequency domain.

The study of the effect of cuff pressure on the measured blood flow and oxygen consumption showed that there is a threshold pressure ( $p_{th} \sim 30$  mm Hg in Figure 5) above which the venous outflow is hindered. Furthermore, at a critical pressure ( $p_c \sim 30$ –45 mm Hg in Figure 5) one achieves a com-

plete venous occlusion. These pressure values were confirmed in the study involving cuff pressure values in the range 15–60 mm Hg.

This result indicates that the effective inflation time in the venous occlusion protocol is the time interval required to increase the cuff pressure from  $p_{th}$  to  $p_c$ . In our measurements this effective inflation time, which is shorter than the inflation time defined in Sec. 3, was in the range 0.2–6.5 s. This time was always shorter than the average time required by the hemoglobin concentration to respond to the venous occlusion (15 s). For this reason, the measured values of BF and OC were shown to be insensitive to the inflation time (see Figure 4).

The spatial maps of blood flow and oxygen consumption in the calf muscle showed a variability of the studied parameters with probe location. The BF and OC values obtained for the spatial maps (Figure 6) are in the range of values shown by the variability of BF and OC values on the same location (see Figure 7). We tested whether this variability could also be attributed to tissue inhomogeneities. In principle, inhomogeneities such as the adipose tissue layer or blood vessels may affect measurements at different locations differently. Our multidistance approach (see the inset of Figure 1) gives optical data at four different source–detector separations ranging from 2.0 to 3.5 cm. Each one of these source–detector separations achieves a different optical penetration depth into the tissue (the larger the source–detector distances, the larger the optical penetration) and probes slightly different tissue volumes. To compare the results from each source–detector pair, we analyzed the data at each source–detector separation using the single-distance, DPF method.<sup>27</sup> In the case shown in Figure 6, we found that the data at each one of the four source–detector distances led to similar values of BF and OC. Consequently, we do not have evidence of the influence of tissue inhomogeneity on the BF and OC measurements shown in Figure 6.

#### 5 Conclusions

Our measurements using different inflation times and cuff pressures show that if the cuff pressure is increased from  $\sim 30$  to  $\sim 45$  mm Hg in less than about 6 s, one records the same values of blood flow and oxygen consumption independent of the total inflation time and final cuff pressure.

The observed increase in the reduced scattering coefficient during venous occlusion suggests that cw spectroscopy may overestimate the occlusion-induced increase in hemoglobin concentration. In fact, the increase in optical density of the calf muscle is partially due to an increase in the scattering coefficient.

The local character of the BF and OC measured using NIRS lends itself to a spatially resolved measurement of the hemodynamics in tissue. In this paper, we have reported proof-of-principle spatial maps of BF and OC in the calf muscle of a human subject. The acquisition time for a spatial map was about 25–30 min because we were performing a venous occlusion for the measurement of the BF and OC values in each pixel. However, a parallel acquisition of the optical data at each image pixel can provide spatial maps of BF and OC in about 1 min, using just one venous occlusion.

## Acknowledgments

This research is supported by the US National Institutes of Health (NIH) Grant No. CA57032, and by Whitaker-NIH Grant No. RR10966.

## References

- I. Ohta, A. Ohta, M. Shibata, and A. Kamiya, *Oxygen Transport to Tissues XII*, M. Mokchizuki et al., Eds., pp. 105–112, Plenum, New York (1988).
- A. Colantuoni, S. Bertuglia, G. Coppini, and L. Donato, *Oxygen Transport to Tissues XII*, Piiper et al., Eds., pp. 549–558, Plenum, New York (1990).
- M. D. Stern, D. L. Lappe, P. D. Bowen, J. E. Chimosky, G. A. Holloway, H. R. Keiser, and R. L. Bowman, "Continuous measurement of tissue blood flow by laser-Doppler spectroscopy," *Am. J. Physiol.* **232**(4), H441–H448 (1977).
- A. D. Edwards, C. Richardson, P. van der Zee, C. Elwell, J. S. Wyatt, M. Cope, D. T. Delpy, and E. O. R. Reynolds, "Measurement of hemoglobin flow and blood flow by near-infrared spectroscopy," *Appl. Physiol.* **75**(4), 1884–1889 (1993).
- M. C. P. van Beekvelt, W. N. J. M. Colier, B. G. M. van Engelen, M. T. E. Hopman, R. A. Wevers, and B. Oeseburg, "Validation of measurement protocols to assess oxygen consumption and blood flow in the human forearm by near infrared spectroscopy," *Proc. SPIE* **3194**, 133–144 (1998).
- R. A. de Blasi, M. Ferrari, A. Natali, G. Conti, A. Mega, and A. Gasparetto, "Noninvasive measurement of forearm blood flow and oxygen consumption by near-infrared spectroscopy," *Appl. Physiol.* **76**(3), 1388–1393 (1994).
- R. A. De Blasi, N. Almenrader, P. Aurisicchio, and M. Ferrari, "Comparison of two methods of measuring forearm oxygen consumption ( $\text{VO}_2$ ) by near infrared spectroscopy," *J. Biomed. Opt.* **2**, 171–173 (1997).
- L. Skov, O. Pryds, G. Greisen, and H. Lou, "Estimation of cerebral venous saturation in newborn infants by near infrared spectroscopy," *Pediatr. Res.* **33**(1), 52–55 (1992).
- C. W. Yoxall and A. M. Weindling, "Measurement of cerebral oxygen consumption in the human neonate using near infrared spectroscopy: cerebral oxygen consumption increases with advancing gestational age," *Pediatr. Res.* **44**(3), 283–289 (1998).
- C. W. Yoxall, A. M. Weindling, N. H. Dawani, and I. Peart, "Measurement of cerebral venous oxyhemoglobin saturation in children by near-infrared spectroscopy and partial jugular venous occlusion," *Pediatr. Res.* **38**(3), 319–323 (1995).
- C. Casavola, L. A. Paunescu, M. A. Franceschini, S. Fantini, L. Winter, J. Kim, D. Wood, and E. Gratton, "Near-infrared spectroscopy and the tilting table protocol: a novel method to study the blood flow and the oxygen consumption in tissues," *Proc. SPIE* **3597**, 685–692 (1999).
- D. M. Mancini, L. Bolinger, H. Li, K. Kendrick, B. Chance, and J. R. Wilson, "Validation of near-infrared spectroscopy in humans," *Am. J. Physiol.* **77**(6), 2740–2747 (1994).
- N. B. Hampson and C. A. Piantadosi, "Near infrared monitoring of human skeletal muscle oxygenation during forearm ischemia," *J. Appl. Physiol.* **64**(6), 2449–2457 (1988).
- T. R. Cheattle, L. A. Potter, M. Cope, D. T. Delpy, P. D. Coleridge Smith, and J. H. Scurr, "Near-infrared spectroscopy in peripheral vascular disease," *Br. J. Surg.* **78**, 405–408 (1991).
- D. J. Wallace, B. Michener, D. Choudhury, M. Levi, P. Fennelly, D. M. Hueber, and B. Barbieri, "Summary of the results of a 90 subject human clinical trial for the diagnosis of peripheral vascular disease using a near-infrared frequency domain hemoglobin spectrometer," *Proc. SPIE* **3597**, 300–316 (1999).
- S. Fantini, B. Barbieri, M. A. Franceschini, and E. Gratton, *Applications of Optical Engineering to the Study of Cellular Pathology*, E. Kohen, Ed., pp. 57–66, Research Signpost, Trivandrum, India (1997).
- S. Fantini, M. A. Franceschini, J. S. Maier, S. A. Walker, B. Barbieri, and E. Gratton, "Frequency-domain multichannel optical detector for noninvasive tissue spectroscopy and oximetry," *Opt. Eng.* **34**(1), 32–42 (1995).
- P. J. O'Brien et al., "Rapid, simple and sensitive microassay for skeletal and cardiac muscle myoglobin and hemoglobin: use in various animals indicates functional role of myogemoproteins," *Mol. Cell. Biochem.* **112**, 45–52 (1992).
- F. A. Duck, *Physical Properties of Tissue: A Comprehensive Reference Book*, p. 321, Academic, San Diego (1990).
- S. Wray, M. Cope, D. T. Delpy, J. S. Wyatt, and E. O. R. Reynolds, "Characterization of the near infrared absorption spectra of cytochrome  $aa_3$  and hemoglobin for the non-invasive monitoring of cerebral oxygenation," *Biochim. Biophys. Acta* **933**, 184–192 (1988).
- W. F. Ganong, "Dynamics of blood & lymph flow," *Review of Medical Physiology*, p. 540, Appleton & Lange, Norwalk (1995).
- W. R. Milnor, *Medical Physiology*, V. B. Mountcastle, Ed., pp. 1033–1046, pp. 1118–1136, The C. V. Mosby Company, St. Louis, MO (1980).
- A. T. Lovell, J. C. Hebden, J. C. Goldstone, and M. Cope, "Determination of the transport scattering coefficient of red blood cells," *Proc. SPIE* **3597**, 175–182 (1999).
- S. Sundberg, "Variation in plethysmographically measured limb blood flow using two study designs," *Chin. Phys.* **15**, 199–206 (1995).
- M. B. Sidery and I. A. Macdonald, "The effect of meal size on the cardiovascular responses to food ingestion," *Br. J. Nutr.* **71**, 835–848 (1994).
- M. Cope, P. van der Zee, M. Essenpreis, S. R. Arridge, and D. T. Delpy, "Data analysis methods for near infrared spectroscopy of tissues: problems in determining the relative cytochrome  $aa_3$  concentration," *Proc. SPIE* **1431**, 251–263 (1991).
- D. T. Delpy, M. Cope, P. van der Zee, S. Arridge, S. Wray, and J. Wyatt, "Estimation of optical pathlength through tissue from direct time of flight measurement," *Phys. Med. Biol.* **33**, 1433–1442 (1988).
- S. Fantini, D. Hueber, M. A. Franceschini, E. Gratton, W. Rosenfeld, P. G. Stubblefield, D. Maulik, and M. R. Stankovic, "Non-invasive optical monitoring of the newborn piglet brain using continuous-wave and frequency-domain methods," *Phys. Med. Biol.* **44**, 1543–1563 (1999).